

# Wedelolactone attenuates sepsis-associated acute liver injury by regulating the macrophage M1/M2 polarization balance through the PI3K/AKT/NF-κB signalling pathway

Wang-Ting Li<sup>1,2#</sup>, Jin-Yi Chen<sup>1,2#</sup>, Shao-Jie Huang<sup>2#</sup>, Dong-Mei Hu<sup>2#</sup>, Xing-Ru Tao<sup>2</sup>, Fei Mu<sup>2</sup>, Jing-Yi Zhao<sup>2</sup>, Chao Guo<sup>2\*</sup>, Jia-Lin Duan<sup>3\*</sup>, Jing-Wen Wang<sup>2\*</sup> 

<sup>1</sup>Department of Pharmacology, Shaanxi University of Chinese Medicine, Xianyang 712046, China. <sup>2</sup>Department of Pharmacy, Xijing Hospital, Fourth Military Medical University, Xi'an 710032, China. <sup>3</sup>Institute of Medical Research, Northwestern Polytechnical University, Xi'an 710032, China.

<sup>#</sup>These authors contributed equally to this work and are co-first authors for this paper.

\*Correspondence to: Chao Guo, Jia-Lin Duan, Jing-Wen Wang. Department of Pharmacy, Xijing Hospital, Fourth Military Medical University, No. 169, Changle West Road, Xi'an 710032, China. E-mail: xysn@163.com; duanjil@nwpu.edu.cn; wangjingwen8021@163.com.

## Author contributions

Jingwen Wang, Jialin Duan and Chao Guo designed and supervised this study. Wangting Li, Jinyi Chen, Shaojie Huang and Dongmei Hu performed the experiments, analyzed the results and wrote the manuscript. Xingru Tao, Fei Mu and Jingyi Zhao assisted in the experiments and revised the article.

## Competing interests

The authors declare no conflicts of interest.

## Acknowledgments

This work was supported by the National Natural Science Foundation of China (No. 81774190, 81903832).

## Peer review information

Traditional Medicine Research thanks all anonymous reviewers for their contribution to the peer review of this paper.

## Abbreviations

ALP, alkaline phosphatase; AST, aspartate aminotransferase; ALT, alanine aminotransferase; AKT, protein kinase B; Arg-1, Arginase 1; CD86, Cluster of Differentiation 86; CD206, Cluster of Differentiation 206; DAPI, 4',6-diamidino-2-phenylindole; SALI, sepsis-associated acute liver injury; DDB, Bifendate; MDA, malondialdehyde; GSH-PX, glutathione peroxidase; IKK, inhibitor of kappa B kinase; IL-6, Interleukin 6; IL-10, Interleukin 10; iNOS, inducible nitric oxide synthase; IκB, inhibitor of kappa B; LPS, lipopolysaccharides; MDA, Malondialdehyde; NF-κB, nuclear factor kappa-B; NO, nitric oxide; PI3K, phosphatidylinositol 3-kinase; P-PI3K, phosphorylated PI3K; P-AKT, phosphorylated AKT; SOD, superoxide dismutase; TNF-α, tumor necrosis factor-α; WED, Wedelactone.

## Citation

Li WT, Chen JY, Huang SJ, et al. Wedelactone attenuates sepsis-associated acute liver injury by regulating the macrophage M1/M2 polarization balance through the PI3K/AKT/NF-κB signalling pathway. *Tradit Med Res*. 2024;9(11):61. doi: 10.53388/TMR20240402001.

Executive editor: Jing-Yi Wang.

Received: 02 April 2024; Accepted: 23 May 2024; Available online: 24 May 2024.

© 2024 By Author(s). Published by TMR Publishing Group Limited. This is an open access article under the CC-BY license. (<https://creativecommons.org/licenses/by/4.0/>)

## Abstract

**Background:** Liver injury caused by sepsis seriously impairs the normal physiology of the liver. Wedelactone (WED) has an obvious anti-inflammatory effect against liver damage caused by various factors. Nevertheless, further research is needed to determine if WED might mitigate acute liver damage linked to sepsis by influencing macrophage polarization. **Methods:** We first assessed the effect of WED on lipopolysaccharides-triggered liver injury by biochemistry assay and tissue staining. Inflammatory factors were assessed using the ELISA kits. The expression of Cluster of Differentiation 86 (CD86) and Cluster of Differentiation 206 (CD206) was measured by immunofluorescence assay. The protein levels of inducible nitric oxide synthase (iNOS), Arginase 1 (Arg-1), phosphatidylinositol 3-kinase (PI3K), protein kinase B (AKT), PI3K phosphorylation (p-PI3K), AKT phosphorylation (p-AKT), inhibitor of kappa B kinase (IKK), inhibitor of kappa B (IκB), and nuclear factor kappa-B (NF-κB) p65 were quantified by western blot analysis. **Results:** WED decreased the level of alanine aminotransferase (ALT), aspartate aminotransferase (AST), alkaline phosphatase (ALP) and malondialdehyde, and increased the activity of superoxide dismutase (SOD) and glutathione peroxidase (GSH-PX). Moreover, WED exerted effective anti-inflammatory effects by decreasing the level of Tumor necrosis factor-α (TNF-α) and Interleukin 6 (IL-6) and increasing the level of Interleukin 10 (IL-10) in serum and cells. WED not only decreased CD86 and iNOS expression but also increased CD206 and Arg-1 expression. WED also downregulated the increased expression of PI3K, AKT, p-PI3K, p-AKT, IKK, and NF-κB p65 induced by lipopolysaccharides, while up-regulated the decreased expression of IκB. Besides, LY294002 with WED decreased the expression of protein PI3K, AKT, p-PI3K, p-AKT, IKK and NF-κB p65, and raised the expression of IκBα. **Conclusion:** Wedelactone could attenuate sepsis-associated acute liver injury, and its mechanism may be associated with balancing pro-inflammatory and anti-inflammatory by the regulation of M1/M2 macrophage polarization via the PI3K/AKT/NF-κB signaling pathway.

**Keywords:** Wedelactone; sepsis; liver injury; macrophage polarization; PI3K/AKT/NF-κB

**Highlights**

Effect of Wedelolactone (WED) on the treatment of sepsis-associated acute liver injury by regulating the macrophage polarization. WED significantly inhibited M1 macrophage polarization by decreasing the expression of Cluster of Differentiation 86 (CD86) and inducible nitric oxide synthase (iNOS), and facilitated M2 macrophage polarization by increasing the expression of Cluster of Differentiation 206 (CD206) and Arginase 1 (Arg-1). WED attenuated lipopolysaccharides-induced acute liver injury by regulating the macrophage polarization through the PI3K/AKT/NF- $\kappa$ B signaling pathway.

**Medical history of objective**

*Eclipta prostrata* (L.) L. is recorded in many ancient Chinese medical books, such as the *Tang Ben Cao* compiled by Su Jing and others in the Tang Dynasty in 659 C.E. WED, a natural coumarin ingredient isolated from *Eclipta prostrata* (L.) L., was used to protect the liver from a variety of liver diseases, including antiviral hepatitis, chemical liver injury, and cholestatic liver injury. Modern pharmacological studies showed that WED has anti-inflammatory, antioxidant, antibacterial and anticancer activities.

**Background**

Sepsis is a potentially fatal organ malfunction, resulting from a compromised host response to infection, according to the latest international consensus in 2016 [1]. Sepsis characterized by high morbidity and mortality covers different age groups, which poses a major danger to human life and health worldwide [2]. In 2017, around 48.9 million individuals were still affected by sepsis, with the disease causing approximately 11 million fatalities [3]. In China, 8.7% of hospitalized sepsis patients occurred in newborns under 1 year old, 11.7% in children 1–9 years old, and 57.5% in elderly people over 65 years old [4]. However, until now, there have been no specific treatments for sepsis, which has greatly limited the prevention and treatment of sepsis [5]. With the progression of severity, sepsis has the potential to induce septic shock and multiple organ dysfunction syndrome, ultimately resulting in patient mortality [6, 7].

During the progression of sepsis, the liver is constantly exposed to a wide range of pathogens, toxins, and inflammatory mediators, which can result in the development of sepsis-associated acute liver injury (SALI) [8]. Without effective intervention and treatment, SALI can further induce liver dysfunction and liver failure [9]. Macrophages maintain internal stability by eliminating pathogenic microorganisms or damaging tissues under physiological conditions, which is closely related to classically activated M1 and alternately activated M2 [10]. When stimulated by persistent severe infection, macrophages are differentiated into M1 macrophages by polarization, which can secrete inflammatory factors to play pro-inflammatory functions [11]. M2 macrophages, known as anti-inflammatory macrophages, play an anti-inflammatory by secreting Interleukin 4 and Interleukin 10 (IL-10) [12]. Therefore, reducing sepsis-associated acute liver injury by regulating macrophage polarization has been regarded as a potential strategy to protect the liver [13].

In clinical practice, antibiotics, intravenous fluids, and vasoconstricting drugs are commonly used to treat sepsis to alleviate or control the source of infection [14]. Among them, early antibiotic treatment is the key measure to treat sepsis. However, with the massive overuse of antibiotics, more and more drug-resistant bacteria have emerged, resulting in poor treatment [15]. Furthermore, there is no specific drug available for the treatment of sepsis so far. It is of great significance to find effective anti-sepsis drugs for clinical treatment. As a natural coumarin ingredient isolated from *Eclipta prostrata* (L.) L., WED has great potential in anti-inflammatory, antioxidant, antibacterial and anticancer activities, which can protect the liver from antiviral hepatitis, chemical liver injury and cholestatic

liver injury [16–18]. Previous studies have found that WED could suppress the expression of caspase-11 induced by lipopolysaccharides (LPS) through suppressing NF- $\kappa$ B-mediated transcription [19]. Nevertheless, whether WED might lessen acute liver damage linked to sepsis by regulating macrophage polarization is currently unclear. The underlying mechanism of the regulation of WED on macrophage polarization remains to be discovered. Thus, we investigated the influence of WED on sepsis-induced acute liver injury caused by LPS by modulating macrophage polarization and explored its potential mechanism.

**Materials and methods****Chemicals and reagents**

Chengdu Pufei De Biotech Co., Ltd. (Chengdu, China) was the supplier of wedelolactone (22031407, Purity 98%). MedChem Express (Monmouth Junction, NJ, USA) provided the Bifendate (DDB, HY-W018791). Sigma-Aldrich (St. Louis, MO, USA) offered the LPS (297-473-0). The alanine transaminase (ALT), aspartate transaminase (AST), and alkaline phosphatase (ALP), malondialdehyde (MDA), superoxide dismutase (SOD), and glutathione peroxidase (GSH-Px) detection kits were purchased from Jiancheng Biotechnology (Nanjing, China) as commercially available kits. Nitric oxide (NO) detection kit was purchased from Beyotime Biotechnology (Beyotime, Shanghai, China). ELISA kits were obtained from Boster Biological Technology (Wuhan, China). Antibodies against CD86 (GB115630-100, 1:1,000) and CD206 (GB115273-100, 1:1,000) were derived from Servicebio Technology Co., Ltd. (Wuhan, China). Antibodies against iNOS (AF0199, 1:1,000), phosphatidylinositol 3-kinase (PI3K) (AF6241, 1:1,000), PI3K phosphorylation (p-PI3K) (AF3241, 1:1,000), Protein kinase B (AKT) (AF0836, 1:1,000), inhibitor of kappa B kinase (IKK) (AF6014, 1:1000) and nuclear factor kappa-B (NF- $\kappa$ B) p65 (AF5006, 1:1,000) were derived from Affinity Biosciences Co., Ltd. (Changzhou, China). Antibodies against AKT phosphorylation (p-AKT) (66444-1-Ig, 1:1,000), Arg-1 (66129-1-Ig, 1:1,000), and inhibitor of kappa B (IkB) (10268-1-AP, 1:1,000) were derived from Wuhan Sanying Biology Technology Co., Ltd. (Wuhan, China).

**Animals and groups**

The Experimental Animal Center of the Fourth Military Medical University (license number: SCX2019-001) provided SPF-grade animal laboratory-fed C57BL/6 mice (male, weighing 20–25 g, aged between 6 and 8 weeks) for this study. The Animal Experiment Ethics Committee of the Fourth Military Medical University approved all involved animal experiments (No. IACUC20230521). All animal experiments were performed in accordance with the guidelines for animal experiments of the Fourth Military Medical University and the National Guide for the Health and Use of Laboratory Animals revised in 1996 (NIH Publication 80-23).

A total of 60 mice were adaptively fed in separate cages for one week. The temperature was controlled at  $22 \pm 2$  °C. The humidity was kept at 55%–75%.

There were 60 mice split into six groups: Control group, LPS group, LPS + 50 mg/kg WED group, LPS + 100 mg/kg WED group, LPS + 200 mg/kg WED group, and LPS + 150 mg/kg DDB group. Mice in WED groups were administered with WED at doses of 50, 100, and 200 mg/kg for seven days, while other mice were only given normal saline continuously for seven days. Mice in the DDB group were gavaged 150 mg/kg DDB for seven days. One hour after the last intragastric administration, all mice except the Control group were injected with 10 mg/kg LPS for 24 h to establish the acute septic liver injury [20]. After the mice were anesthetized with pentobarbital intraperitoneally, serum and liver tissue were obtained for subsequent analysis.

**Serum biochemical analysis**

Commercial test kits were employed to measure the concentration of ALT, AST, and ALP in serum.

### ELISA analysis

The levels of Tumor necrosis factor- $\alpha$  (TNF- $\alpha$ ), Interleukin 6 (IL-6), and IL-10 were measured in both serum and cell samples using the ELISA kits.

### Analysis of the antioxidant system

According to the instructions of commercial kits, the liver tissue supernatant was used to detect SOD and GSH-PX activity and MDA content.

### Histological analysis

4% paraformaldehyde was utilized to fix liver tissue for 24 h. After gradient dehydration with ethanol, fresh liver tissue specimens were embedded in paraffin blocks and then sliced to obtain 4  $\mu$ m paraffin sections. Next, the H&E staining was performed on the paraffin sections. The images were seen and obtained with an Olympus BX43 microscope (Tokyo, Japan).

### Liver immunofluorescence assay

4  $\mu$ m paraffin sections from liver tissue were incubated with anti-CD86, anti-CD206 and anti-F4/80 overnight. After that, they were cultured at room temperature in the absence of light for one hour, using goat anti-rabbit secondary antibody that had been labelled with horseradish peroxidase (HRP). The nucleus was stained with 4',6-diamidino-2-phenylindole (DAPI) for 8–10 min. A confocal laser scanning microscope was used to capture the images (ECLIPSE Ti-E and Ti-E/B, Nikon, Tokyo, Japan). Semi-quantitative fluorescence analysis was performed by Image J software.

### Molecular docking

The 2D structure of WED was processed by Schrödinger to generate 3D chiral conformation. The crystal structures of PI3K and AKT proteins were obtained from the RCSB PDB database (<https://www.rcsb.org/>) and further processed by Schrödinger to obtain the active site of the proteins. Molecular docking of the treated compound Wedelolactone to the active site of the proteins was performed and the binding free energy was analyzed by MM-GBSA calculation and analysis.

### Cell cultures and treating

RAW264.7 cells were cultured in DMEM with 10% fetal bovine serum (Procell, Wuhan, China) and 1% antibiotic (Solarbio, Beijing, China) at a temperature of 37 °C with a CO<sub>2</sub> concentration of 5% in a humidified environment. To establish the model group, 1  $\mu$ g/mL of LPS dissolved in 0.1% dimethyl sulfoxide was introduced to the cell culture medium for 24 h [13]. For the treatment groups, multiple concentrations of WED were supplemented to RAW264.7 cells along with LPS for 24 h. The control group consisted solely of RAW264.7 cells cultured in DMEM for 24 h without any additional substances or treatments applied.

### Cell viability

The cell viability was performed using a CCK-8 kit (Topscience, Shanghai, China). RAW264.7 cells were cultured in DMEM at a density of  $5 \times 10^4$  cells/well and treated with varying concentrations (1.25, 2.5, 5, 10, 20, 40, 80, and 160  $\mu$ M) of WED for 24 h. Absorbance values at 450 nm were detected using the microplate reader from Bio-Rad Laboratories (Hercules, CA, USA).

### No production

NO production in RAW264.7 cells was detected according to the instructions of the NO assay kit (Beyotime, Shanghai, China).

### Cell immunofluorescence assay

The RAW264.7 cells were inoculated with the density of  $1 \times 10^5$  cells/well, following incubated for 24 h. Following exposure to different stimuli, the cells were fixed using 4.0% p-formaldehyde and permeabilized including Triton X-100 (Beyotime, Shanghai, China).

Subsequently, Immunol Staining Blocking Buffer (Beyotime, Shanghai, China) was applied for 30 min, followed by incubation with diluted primary antibodies at 4 °C for several hours. Then RAW264.7 cells were exposed to Alexa Fluor 488-labeled IgG secondary antibody (Beyotime, Shanghai, China). Finally, DAPI staining was performed on the nucleus using a volume of 500  $\mu$ L for 8–10 min. The resulting images were observed utilizing a confocal laser scanning microscope (ECLIPSE Ti-E and Ti-E/B, Nikon, Japan) and analyzed by Image J software.

### Western blot analysis

The proteins from liver tissues and RAW264.7 cells were obtained according to a protein extraction kit. The concentrations of proteins were measured by the BCA Protein Assay kit (Beyotime, Shanghai, China). Subsequently, 40  $\mu$ g of total proteins were separated through 10% sodium dodecyl-sulfate-polyacrylamide gel electrophoresis (Beyotime, Shanghai, China) and subsequently transferred onto a PVDF membrane (Merck Millipore, Billerica, MA, USA). To block the membranes for further analysis at room temperature for 2 h in  $1 \times$  Tris-buffered saline (Servicebio, Wuhan, China) with 0.1% Tween-20 (Solarbio, Beijing, China), a solution of 5% skim milk was employed. Following this step, the primary antibodies were incubated at 4 °C overnight. Room temperature incubation with secondary antibodies was performed for an additional two hours. Finally, image-analysis systems (Bio-Rad, Hercules, CA, USA) were used to capture the images while Image J software was used to analyze the protein bands.

### Statistical analysis

The data were presented as mean  $\pm$  standard deviation and analyzed using GraphPad Prism 8.0.2. To determine the statistical variances among different groups, One-way ANOVA and Tukey's multiple comparison tests were performed.

## Results

### Wedelolactone alleviated LPS-induced liver injury in mice

When the liver is injured, the markers ALT, AST, and ALP are abnormally elevated, which are always used to determine the extent of liver damage. As shown in Figure 1A–1C, ALT, AST and ALP in serum were significantly elevated compared to the Control group when the mice were injected with LPS to induce acute liver injury ( $P < 0.01$ ). However, WED substantially reduced the elevation of ALT, AST, and ALP ( $P < 0.01$ ). Similarly, HE staining was also used to observe the damage degree of the liver structure. As shown in Figure 1D, the structure of the hepatic lobule in the control group was clear and complete. In addition, no inflammatory cell infiltration was observed. In the LPS group, the structure of the hepatic lobule was severely damaged, including necrosis of hepatocytes, inflammatory infiltration, and vacuolation of hepatocytes. With the increasing dosage of WED, the above symptoms of liver injury were effectively improved, especially at the high dosage of WED. MDA concentration, SOD and GSH-PX activities were measured to reflect oxidative stress in liver tissue (Figure 1E–1G). Compared with the Control group, the LPS group exhibited a significant increase in MDA concentration and a decrease in SOD and GSH-PX activity ( $P < 0.01$ ). Conversely, WED markedly reduced the assessed MDA concentration and enhanced SOD and GSH-PX activity ( $P < 0.01$ ). Thus, the results indicated that WED alleviated the effects of LPS-induced acute liver injury in mice.

### Wedelolactone attenuated inflammatory reaction by adjusting macrophage polarization in the liver

When the liver is injured, it produces an enormous quantity of cytokines, triggering an inflammatory response. As shown in Figure 2A, 2B, the levels of TNF- $\alpha$  and IL-6 in the LPS group were considerably higher than those in the Control group ( $P < 0.01$ ). However, in the WED groups, they were fully lower compared to the LPS group ( $P < 0.01$ ). Furthermore, Macrophage polarization was detected by immunofluorescence staining of liver tissue. After liver induction with LPS, the expression of CD86 involved with M1



macrophage polarization was strengthened remarkably, but the expression of CD206 related to M2 macrophage polarization was decreased notably (Figure 2C, 2E). Furthermore, WED treatment diminished CD86 expression and raised CD206 expression compared with LPS group. The results of fluorescence semi-quantitative analysis of CD86 and CD206 were consistent with the observed images (Figure 2D, 2F). The expression of protein iNOS and Arg-1, reflecting M1 macrophage polarization and M2 macrophage polarization, were further examined by western blotting. Under the stimulation of LPS, the expression of protein iNOS was decreased observably, whereas the expression of protein Arg-1 was increased remarkably (Figure 2G–2I). However, WED treatment significantly promoted LPS-induced

decreased protein expression of Arg-1. The abnormal protein expression of iNOS induced by LPS was suppressed after WED intervention. These results indicated that WED could decline the levels of TNF- $\alpha$  and IL-6 by inhibiting M1 macrophage polarization and activating M2 macrophage polarization in response to inflammatory cytokines in the liver.

#### Wedelolactone regulated macrophage polarization through PI3K/AKT/NF- $\kappa$ B signaling pathway in the liver

As shown in Supplementary Table 1, the docking scores of WED with PI3K and AKT were  $-8.991$  and  $-9.558$ , respectively. Meanwhile, the results of MM-GBSA analysis were  $-28.46$  kcal/mol and  $-51.93$

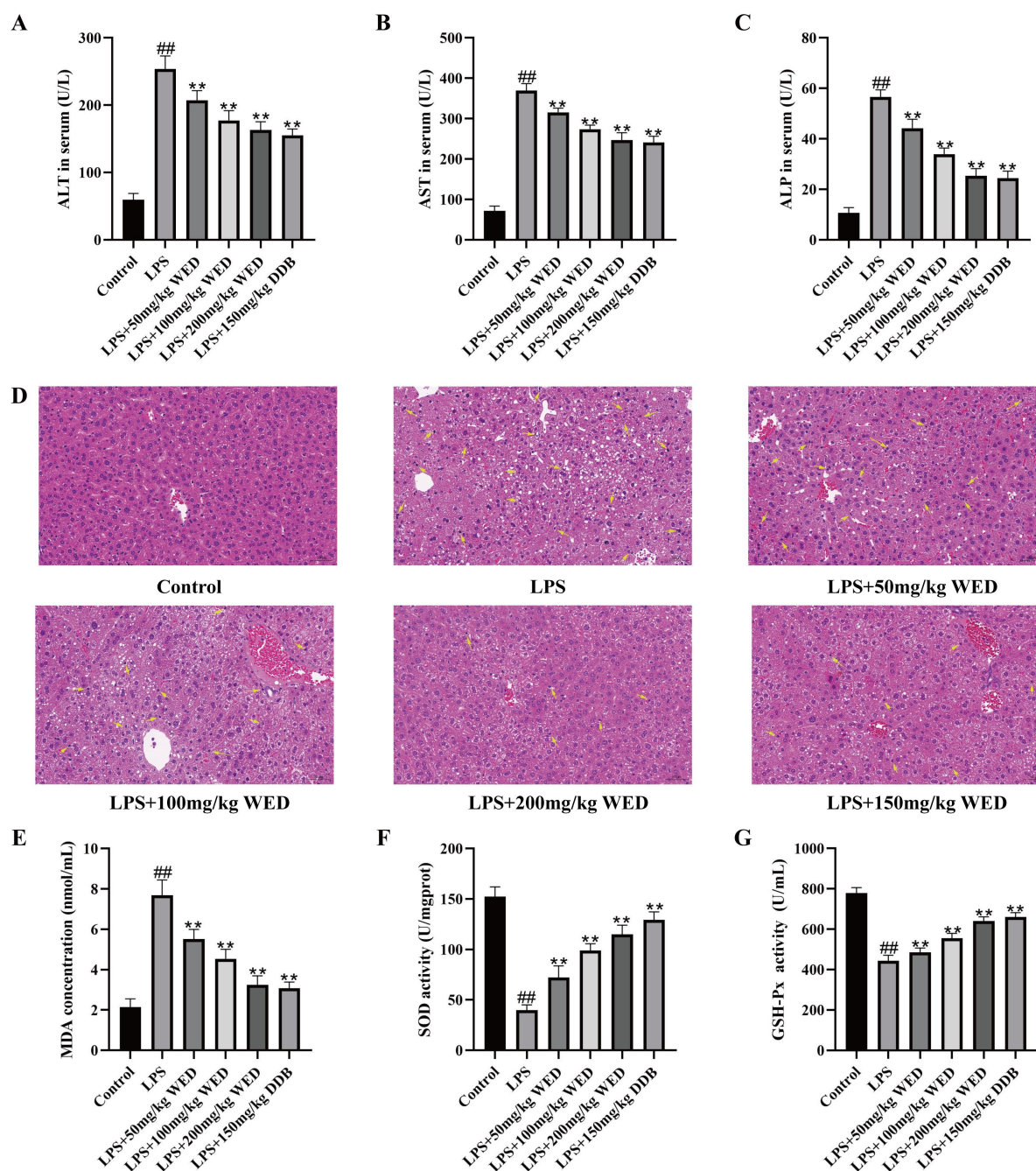


**Figure 1** Wedelolactone alleviated LPS-induced liver injury in mice. (A–C) ALT, AST and ALP in serum were detected ( $n = 6$ ). (D) The damage degree of liver structure was observed by H&E staining. Scale bar: 50  $\mu$ m ( $n = 3$ ). (E–G) MDA, SOD and GSH-Px in the liver were examined ( $n = 6$ ). <sup>##</sup> $P < 0.01$  vs Control group, <sup>\*\*</sup> $P < 0.01$  vs LPS group. ALP, alkaline phosphatase; AST, aspartate aminotransferase; ALT, alanine aminotransferase; LPS, lipopolysaccharides; DDB, Bifendate; WED, Wedelactone; MDA, malondialdehyde; GSH-Px, glutathione peroxidase; SOD, superoxide dismutase.

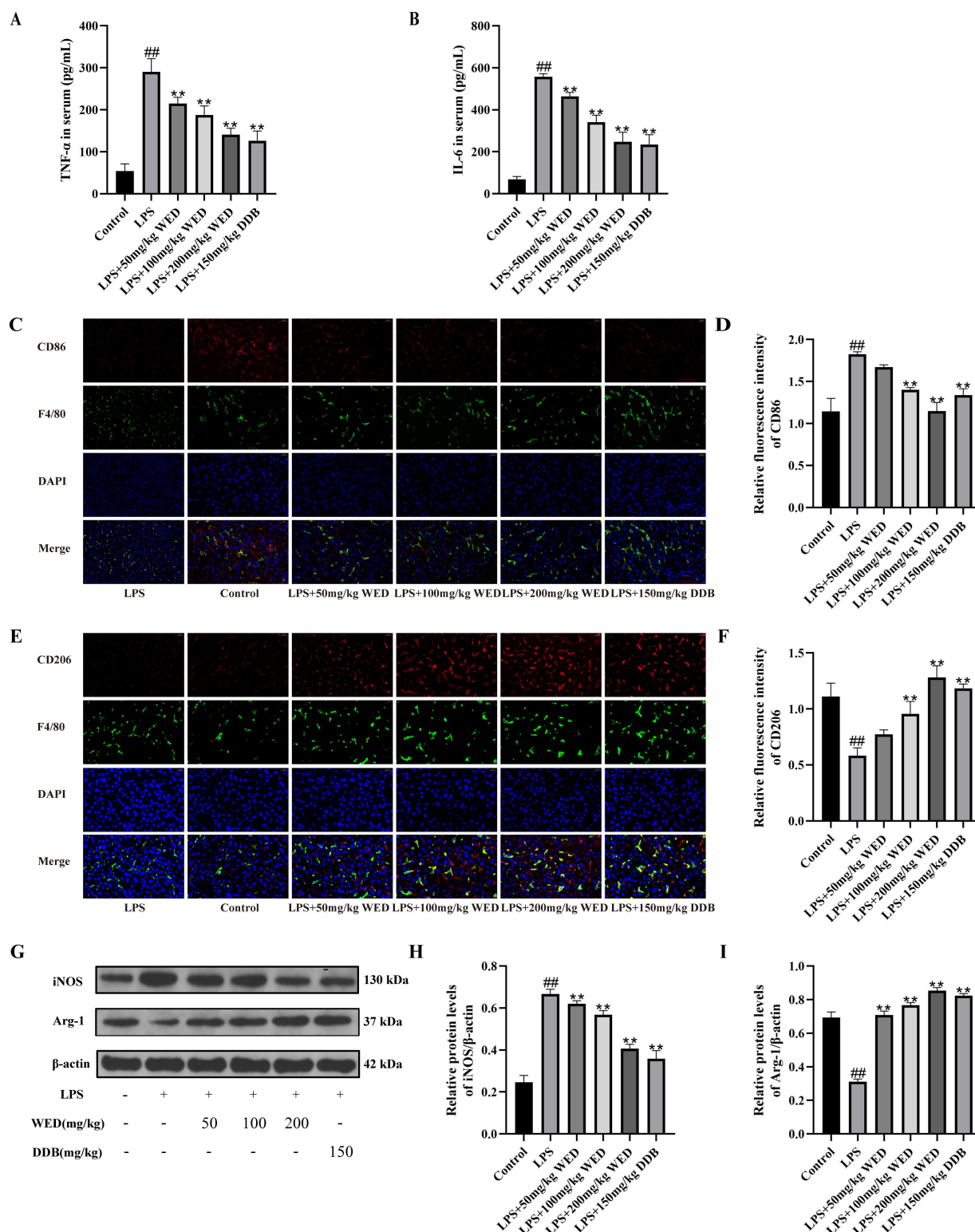


**Figure 2** Wedelolactone attenuated inflammatory response by regulating macrophage polarization in the liver. (A, B) ELISA kit detected levels of inflammatory factors in serum ( $n = 6$ ). (C) CD86 expression were measured by immunofluorescence assay in the liver, Scale bar: 20  $\mu\text{m}$  ( $n = 3$ ). (D) Semi-quantitative immunofluorescence analysis of CD86, Scale bar: 20  $\mu\text{m}$  ( $n = 3$ ). (E) CD206 expression were measured by immunofluorescence assay in the liver, Scale bar: 20  $\mu\text{m}$  ( $n = 3$ ). (F) Semi-quantitative immunofluorescence analysis of CD206 ( $n = 3$ ). (G–I) iNOS and Arg-1 protein expression were determined by western blotting in the liver ( $n = 3$ ). <sup>##</sup> $P < 0.01$  vs Control group, <sup>\*\*</sup> $P < 0.01$  vs LPS group. TNF- $\alpha$ , tumor necrosis factor- $\alpha$ ; IL-6, Interleukin 6; LPS, lipopolysaccharides; DDB, Bifendate; WED, Wedelactone; CD86, Cluster of Differentiation 86; CD206, Cluster of Differentiation 206; DAPI, 4',6-diamidino-2-phenylindole; iNOS, inducible nitric oxide sythase; Arg-1, Arginase 1.

kcal/mol, respectively. Both the docking scores and the binding free energy were very low, indicating that WED bound to PI3K/AKT very stably (Figure 3A, 3B). To further explore how WED regulates

macrophage polarization in the liver, the expression of proteins corresponding with the PI3K/AKT/NF- $\kappa\text{B}$  signaling was detected. The expression of PI3K, AKT, p-PI3K and p-AKT were significantly

up-regulated under the stimulation of LPS in the liver (Figure 3C–3E). In contrast, WED significantly downregulated the expression of PI3K, AKT, p-PI3K and p-AKT. Additionally, to the influence of WED on macrophage polarization via the adjustment of NF- $\kappa$ B, the protein levels of IKK, I $\kappa$ B, and NF- $\kappa$ B p65 were also examined by western blotting. In the LPS group, the protein level of IKK and NF- $\kappa$ B p65 were up-regulated, whereas the protein level of I $\kappa$ B $\alpha$  was downregulated (Figure 3F–3I). Compared with the LPS group, WED administration markedly reversed the decrease of I $\kappa$ B $\alpha$  expression and the increase of IKK and NF- $\kappa$ B p65. Thus, these results indicated that WED regulated macrophage polarization in response to LPS-stimulated liver by suppressing the PI3K/AKT/ NF- $\kappa$ B pathway.

#### Wedelolactone suppressed inflammation caused by LPS in RAW264.7 cells.

The chemical structure of WED was shown in Figure 4A. The effect of WED on the viability of Raw264 cells was assessed using CCK8. When RAW264.7 cells were exposed to WED concentrations below 40 mol/L for 24 h, no observable effect on cell viability was observed (Figure

4B). Furthermore, RAW264.7 cells were treated with WED at concentrations ranging from 2.5  $\mu$ M to 40  $\mu$ M to investigate its influence on LPS-induced NO production. While there was no significant increase in NO production in RAW264.7 cells stimulated by LPS, the growth of NO concentration was effectively restricted by WED treatment (Figure 4C). Consequently, we selected WED concentrations of 10, 20, and 40  $\mu$ M for subsequent experiments aiming to explore its anti-inflammatory effects. Subsequent analysis revealed that stimulation of RAW264.7 cells with LPS led to a noticeable elevation in levels of TNF- $\alpha$ , IL-6, and IL-10 (Figure 4D–4F). However, treatment with WED significantly suppressed the production of TNF- $\alpha$  and IL-6, and markedly promoted the expression of IL-10.

Then, we demonstrated the effects of WED on LPS-induced macrophage polarization markers by immunofluorescence assay and western blotting, such as CD86 and CD206. The expression level of CD86 showed a noticeable increase, while the expression level of CD206 exhibited a significant decrease (Figure 4G). Surprisingly, WED reversed the LPS-induced expression of CD86 and CD206. The relative

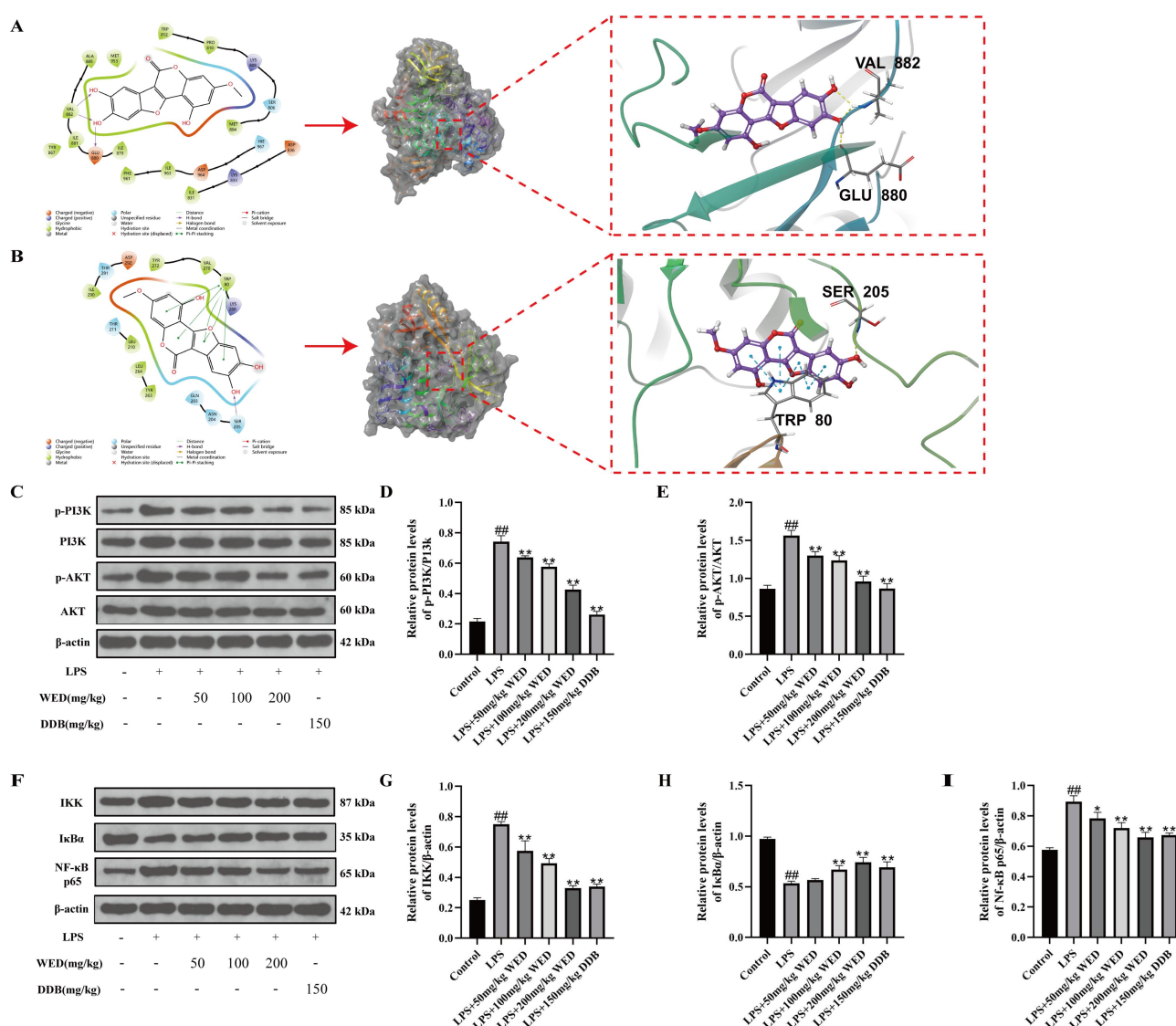


**Figure 3** Wedelolactone regulated macrophage polarization via PI3K/AKT/NF- $\kappa$ B pathway. (A) 2D and 3D images of WED docking with PI3K protein. (B) 2D and 3D images of WED docking with AKT protein. (C–I) The effects of WED on protein expression in LPS-induced liver were determined (n = 3).  $^{##}P < 0.01$  vs Control group,  $^{*}P < 0.05$ ,  $^{**}P < 0.01$  vs LPS group. PI3K, phosphatidylinositol 3-kinase; P-PI3K, phosphorylated PI3K; P-AKT, phosphorylated AKT; AKT, protein kinase B; LPS, lipopolysaccharides; DDB, Bifendate; WED, Wedelactone; IKK, inhibitor of kappa B kinase; I $\kappa$ B, inhibitor of kappa B; NF- $\kappa$ B, nuclear factor kappa-B.



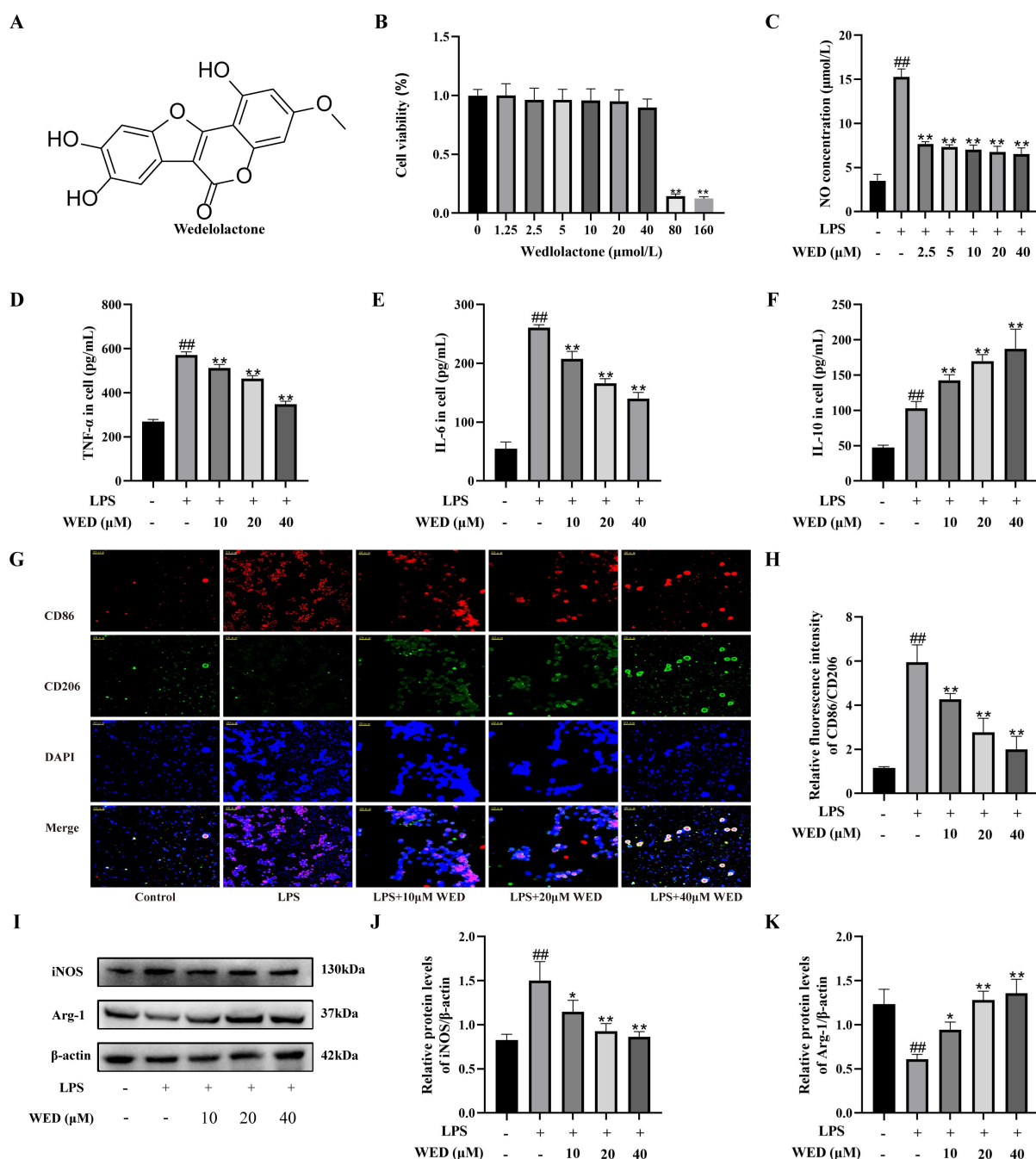


**Figure 4** Wedelolactone suppressed inflammation caused by LPS in RAW264.7 cells. (A) The structure of Wedelolactone. (B) CCK-8 kit detected cell viability ( $n = 6$ ). (C) NO production was detected ( $n = 6$ ). (D–F) ELISA kit detected levels of inflammatory factors ( $n = 6$ ). (G) CD86 and CD206 expression were observed by immunofluorescence assay, Scale bar: 20  $\mu\text{m}$  ( $n = 3$ ). (H) Semi-quantitative immunofluorescence analysis of CD86/CD206 ( $n = 3$ ). (I–K) iNOS and Arg-1 protein expression were determined by western blotting ( $n = 3$ ).  $^{##}P < 0.01$  vs Control group,  $^{*}P < 0.05$ ,  $^{**}P < 0.01$  vs LPS group. iNOS, inducible nitric oxide synthase; Arg-1, Arginase 1; LPS, lipopolysaccharides; WED, Wedelolactone; CD206, Cluster of Differentiation 206; DAPI, 4',6-diamidino-2-phenylindole; TNF- $\alpha$ , tumor necrosis factor- $\alpha$ ; IL-6, Interleukin 6; IL-10, Interleukin 10; NO, nitric oxide.

fluorescence intensity analysis of CD86/CD206 showed that the fluorescence intensity increased in response to LPS and decreased significantly after WED administration (Figure 4H). Subsequently, the protein levels of iNOS and Arg-1 were analyzed by western blotting. Following the observations in vivo, the increase of iNOS and reduction of Arg-1 were also observed when RAW264.7 cells were exposed to LPS (Figure 4I–4K). The above results indicated that WED played an anti-inflammatory role by regulating of M1/M2 macrophage polarization balance in LPS-stimulated RAW264.7 cells.

#### Wedelolactone regulated macrophage polarization via

Submit a manuscript: <https://www.tmrjournals.com/tmr>

#### PI3K/AKT/NF- $\kappa$ B signaling pathway in vitro

The western blotting technique was employed to quantify the relevant proteins to investigate the impact of WED on Macrophage polarization in RAW264.7 cells induced by LPS, specifically through the PI3K/AKT/NF- $\kappa$ B signaling pathway. Upon stimulation with LPS, there was a noticeable increase in the protein levels of PI3K, AKT, p-PI3K, and p-AKT (Figure 5A–5C). Conversely, WED effectively reduced these protein levels. Likewise, WED effectively downregulated the protein level of PI3K, AKT, p-PI3K and p-AKT. Next, we determined the level of IKK, I $\kappa$ B and NF- $\kappa$ B p65 in RAW264.7 cells induced by LPS. These findings indicated that LPS stimulation led

to an evident elevation in IKK and NF- $\kappa$ B p65 levels while decreasing I $\kappa$ B levels (Figure 5D–5G). Moreover, administration of WED significantly reduced the protein levels of IKK and NF- $\kappa$ B p65 compared to LPS stimulation alone; meanwhile, it notably increased I $\kappa$ B expression level. Taken together, these findings demonstrated that WED modulated Macrophage polarization via activation of the PI3K/AKT/NF- $\kappa$ B signaling pathway in RAW264.7 cells induced by LPS.

#### LY294002 enhanced the effect of WED on M1/M2 macrophages polarization

To confirm whether PI3K/AKT/NF- $\kappa$ B mediated the effects of WED on M1/M2 macrophages polarization, PI3K/AKT pathway inhibitor (LY294002) was used to observe the changes. Due to 40  $\mu$ M WED exerted great anti-inflammatory effects and regulatory effects on M1/M2 macrophage polarization, we selected it with LY294002 for the following experiments. The expression levels of TNF- $\alpha$  and IL-6 in RAW264.7 cells induced by LPS were significantly inhibited by LY294002, while the expression of IL-10 was promoted (Figure 6A–6C). Moreover, this trend became more pronounced when RAW264.7 cells were treated with WED and LY294002. It was observed that CD86 expression and relative fluorescence intensity of CD86/CD206 decreased dramatically with the LY294002 treatment, whereas CD206 expression increased (Figure 6D, 6E). Consequently, these results indicated that the effect of WED on M1/M2 macrophage polarization was further augmented by LY294002.

#### LY294002 enhanced the effect of WED on inhibiting the PI3K/AKT/NF- $\kappa$ B signaling pathway

Subsequently, we conducted further analysis on the protein expression associated with the PI3K/AKT/NF- $\kappa$ B pathway in RAW264.7 cells treated with WED or LY294002 after LPS induction. The levels of PI3K, AKT, p-PI3K, and p-AKT proteins were significantly reduced in RAW264.7 cells following induction with LPS and LY294002 (Figure 7A–7C). Additionally, co-treatment of WED and LY294002 resulted in decreased expression of PI3K, AKT, p-PI3K, and p-AKT proteins, leading to the inhibition of PI3K/AKT pathway activation. Moreover, there was a remarkable decrease in IKK and NF- $\kappa$ B p65 protein levels observed while the expression level of I $\kappa$ B $\alpha$  protein was noticeably increased (Figure 7D–7G). Henceforth, these findings indicated that during LPS stimulation in RAW264.7 cells, LY294002 enhanced the suppressive effect of WED on PI3K/AKT/NF- $\kappa$ B activation.

#### Discussion

Recent studies have indicated that sepsis can be caused by various types of infections, such as bacteria, viruses, fungi, and parasites. This condition can result in damage to multiple organs such as the liver, kidneys, and brain [21]. Both Gram-negative and Gram-positive bacteria have been identified as potential culprits for causing sepsis [22]. The occurrence of sepsis is often initiated by a crucial component found in the cell wall of gram-negative bacteria known as LPS [23]. Therefore, we used LPS to induce SALI and inflammatory reaction in RAW264.7 cells in vitro, respectively. Our results suggested that the levels of ALT, AST, and ALP were elevated after the mice were injected with LPS. In contrast, WED administration prompted an impressive reduction in the level of ALT, AST, and ALP. Furthermore, WED improved LPS-induced hepatocyte necrosis, inflammatory infiltration and hepatocyte vacuolation, indicating that WED could effectively alleviate acute liver injury induced by LPS in mice.

Hepatic macrophages exert an extremely important part in the initiation, maintenance and recovery of liver inflammation and damage in many liver diseases such as viral hepatitis, liver fibrosis and fatty liver disease [24, 25]. When the pathogen invades the liver, stellate cells, kupffer cells, liver sinusoidal endothelial cells, and so on, are involved in clearing bacteria and mediating inflammatory responses to defend and prevent sepsis-associated acute liver injury [26]. As the largest tissue-resident macrophage, kupffer cells located in the hepatic sinuses were activated and differentiated into different phenotypes to trigger an inflammatory response [27]. On the one hand, macrophages in the resting state are activated and differentiated into the M1 phenotype under the stimulation of LPS, which eliminates pathogenic microorganisms by secreting pro-inflammatory cytokines [28]. In our study, TNF- $\alpha$  and IL-6 levels in serum and RAW264.7 cells were increased. However, the overwhelming expression of pro-inflammatory cytokines not only fails to alleviate LPS-induced inflammation but causes further damage to the liver. Pretreatment WED observably inhibited the increase of TNF- $\alpha$  and IL-6. On the other hand, M2 macrophages, known as anti-inflammatory macrophages, exert great anti-inflammatory effect by secreting IL-10 [29]. We observed the increase of IL-10 in LPS-induced RAW264.7 cells, which was further dramatically increased with the increase of WED concentration.

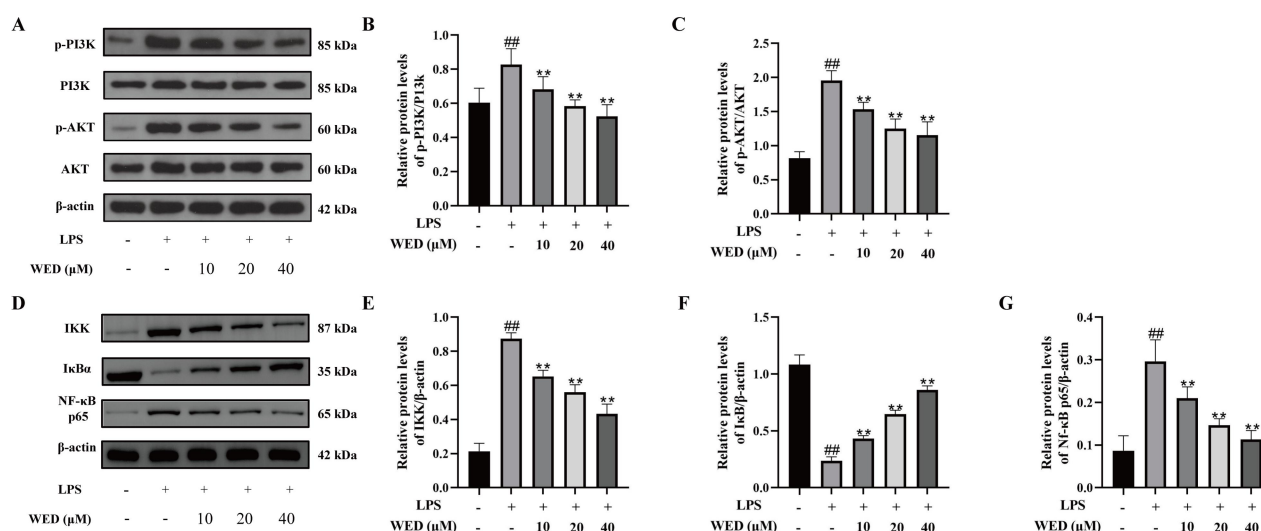


**Figure 5** Wedelolactone regulated macrophage polarization via PI3K/AKT/NF- $\kappa$ B signaling pathway in LPS-induced RAW264.7 cells. (A–G) The effects of WED on protein expression in LPS-induced RAW264.7 cells (n = 3).  $^{##}P < 0.01$  vs Control group,  $^{**}P < 0.01$  vs LPS group. LPS, lipopolysaccharides; WED, Wedelactone; PI3K, phosphatidylinositol 3-kinase; P-PI3K, phosphorylated PI3K; P-AKT, phosphorylated AKT; AKT, protein kinase B; IKK, inhibitor of kappa B kinase; I $\kappa$ B, inhibitor of kappa B; NF- $\kappa$ B, nuclear factor kappa-B.



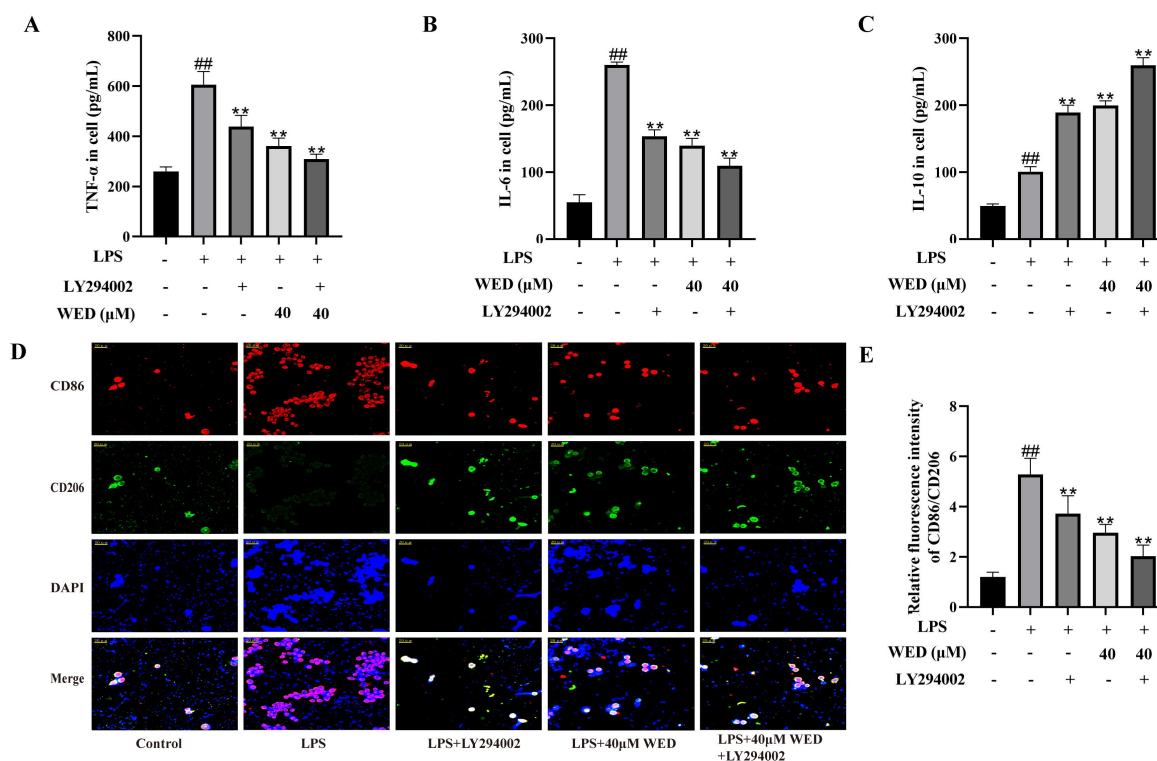


**Figure 6** LY294002 enhanced the effect of WED on M1/M2 macrophages polarization. (A–C) ELISA kit detected levels of inflammatory factors ( $n = 6$ ). (D) CD86 and CD206 expression were observed by immunofluorescence assay, Scale bar: 20  $\mu$ m ( $n = 3$ ). (E) Semi-quantitative immunofluorescence analysis of CD86/CD206 ( $n = 3$ ). <sup>##</sup> $P < 0.01$  vs Control group, <sup>\*\*</sup> $P < 0.01$  vs LPS group. TNF- $\alpha$ , tumor necrosis factor- $\alpha$ ; IL-6, Interleukin 6; IL-10, Interleukin 10; LPS, lipopolysaccharides; WED, Wedelactone; CD86, Cluster of Differentiation 86; CD206, Cluster of Differentiation 206.

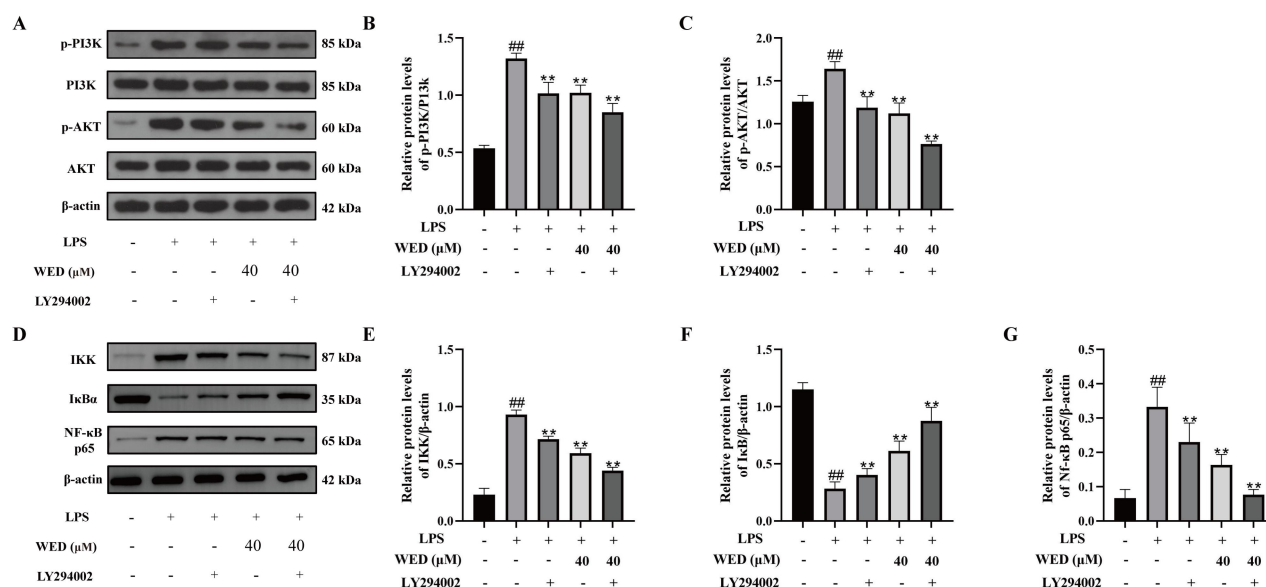


**Figure 7** LY294002 enhanced the effect of WED on inhibiting the PI3K/AKT/NF- $\kappa$ B signaling pathway. (A–G) Representative bands and quantitative of PI3K, AKT, NF- $\kappa$ B and IKK in LPS-induced RAW264.7 cells ( $n = 3$ ). <sup>##</sup> $P < 0.01$  vs Control group, <sup>\*\*</sup> $P < 0.01$  vs LPS group. LPS, lipopolysaccharides; WED, Wedelactone; PI3K, phosphatidylinositol 3-kinase; P-PI3K, phosphorylated PI3K; P-AKT, phosphorylated AKT; AKT, protein kinase B; IKK, inhibitor of kappa B kinase; I $\kappa$ B, inhibitor of kappa B; NF- $\kappa$ B, nuclear factor kappa-B.

Macrophage polarization participated in the pathophysiological processes of different tissues, such as inflammation, tumor, tissue repair and metabolism, which played different regulatory functions in response to different stimuli [30]. Regulating macrophage polarization by adjusting M1/M2 macrophage polarization was considered as a new strategy to limit the production of inflammatory factors and promote tissue repair [31, 32]. We first detected M1 and M2 macrophage expression markers CD86 and CD206 by

immunofluorescence assay respectively and found that stimulation with LPS substantially increased CD86 expression and reduced CD206 expression in liver and RAW264.7 cells. However, WED significantly countered the elevation of CD86 and reduction of CD206 in a dose-dependent manner. Besides, iNOS could be expressed by M1 macrophages, which reflects M1 macrophage polarization [33]. Similarly, anti-inflammatory Arg-1 produced by M2 macrophages was one of the markers of M2 macrophage polarization [34]. Western

blotting revealed that LPS-stimulated liver and RAW264.7 cells expressed more iNOS and less Arg-1, while WED treatment remarkably suppressed both of these changes. These data suggested that WED attenuated LPS-induced inflammation by regulating macrophage M1/M2 polarization balance.

Previous data revealed that the involvement of the PI3K/AKT signaling pathway participated in LPS-induced inflammatory reactions and acute tissue injuries such as lung, kidney, and liver [35–37]. Meanwhile, as one of the most important regulation pathways, PI3K/AKT is essential for the process of macrophage polarization [38]. The western blotting results demonstrated that LPS-triggered high expression of PI3K, AKT, p-PI3K, and p-AKT in the liver was inhibited by WED. Consistent with the results in vivo, the expression levels of PI3K, AKT, p-PI3K and p-AKT after WED intervention were lower than LPS stimulation in RAW264.7 cells. Moreover, NF- $\kappa$ B transcription factor is an important regulator of the immune system, which plays anti-apoptotic, pro-proliferative and pro-inflammatory roles under different stimuli [39]. Accumulating evidence has demonstrated that sepsis-induced tissue injury could be effectively attenuated by suppressing M1 macrophage polarization by preventing activation of the NF- $\kappa$ B pathway [40]. The activation of the NF- $\kappa$ B signaling pathway was initiated by inducing phosphorylation of IKK and subsequent degradation of I $\kappa$ B protein. This led to a significant release of pro-inflammatory mediators such as TNF- $\alpha$ , IL-1 $\beta$ , and NO [38]. The levels of IKK and NF- $\kappa$ B p65 were greatly increased in response to LPS, while the level of I $\kappa$ B showed an abnormal decrease. Importantly, WED exhibited anti-inflammatory properties by preventing the expression of IKK and NF- $\kappa$ B p65 induced by LPS. Additionally, it effectively inhibited the degradation of I $\kappa$ B $\alpha$ . These findings suggest that WED has potential as an anti-inflammatory agent through its ability to inhibit NF- $\kappa$ B activation.

To confirm whether the effects of WED on M1/M2 macrophages polarization in RAW264.7 cells were enhanced, LY294002 was used to further examine the level of inflammatory factors and the protein expression associated with macrophage polarization. As we expected, LY294002 with WED exerted anti-inflammatory effects by lowering TNF- $\alpha$  and IL-6 expression and raising IL-10 expression in RAW264.7 cells stimulated by LPS. Subsequently, we detected the protein expression of the PI3K/AKT/NF- $\kappa$ B signaling pathway when RAW264.7 cells were intervened with LY294002 and LPS. LY294002 with WED downregulated the expression of PI3K, AKT, p-PI3K, p-AKT, IKK, and NF- $\kappa$ B p65, while up-regulated the expression of I $\kappa$ B. Surprisingly, this effect was similar to LY294002 combined with LPS, directly indicating that WED regulated macrophage polarization by suppressing activation of the PI3K/Akt/NF- $\kappa$ B pathway.

In summary, our data suggested that Wedelolactone attenuated sepsis-associated acute liver injury by suppressing M1 macrophage polarization and facilitating M2 macrophage polarization via PI3K/AKT/NF- $\kappa$ B signaling pathway. However, multi-factor interaction affects macrophage polarization, which is a complex process involving a variety of signaling molecules and their pathways. The effects of WED on macrophage polarization through other signaling pathways still need further experimental research.

## References

- Singer M, Deutschman CS, Seymour CW, et al. The third international consensus definitions for sepsis and septic shock (Sepsis-3). *JAMA*. 2016;315(8):801. Available at: <http://doi.org/10.1001/jama.2016.0287>
- Tillmann B, Wunsch H. Epidemiology and Outcomes. *Crit Care Clin*. 2018;34(1):15–27. Available at: <http://doi.org/10.1016/j.ccc.2017.08.001>
- Rudd KE, Johnson SC, Agesa KM, et al. Global, regional, and national sepsis incidence and mortality, 1990–2017: analysis for the Global Burden of Disease Study. *Lancet*. 2020;395(10219):200–211. Available at: [http://doi.org/10.1016/S0140-6736\(19\)32989-7](http://doi.org/10.1016/S0140-6736(19)32989-7)
- Weng L, Xu Y, Yin P, et al. National incidence and mortality of hospitalized sepsis in China. *Crit Care*. 2023;27(1):84. Available at: <http://doi.org/10.1186/s13054-023-04385-x>
- Cohen J, Vincent JL, Adhikari NKJ, et al. Sepsis: a roadmap for future research. *Lancet Infect Dis*. 2015;15(5):581–614. Available at: [http://doi.org/10.1016/S1473-3099\(15\)70112-X](http://doi.org/10.1016/S1473-3099(15)70112-X)
- Lever A, Mackenzie I. Sepsis: definition, epidemiology, and diagnosis. *BMJ*. 2007;335(7625):879–883. Available at: <http://doi.org/10.1136/bmj.39346.495880.AE>
- Zhang H, Feng YW, Yao YM. Potential therapy strategy: targeting mitochondrial dysfunction in sepsis. *Mil Med Res*. 2018;5(1):41. Available at: <http://doi.org/10.1186/s40779-018-0187-0>
- Yao YW, Wang DM, Yin YM. Advances in sepsis-associated liver dysfunction. *Burns Trauma*. 2014;2(3):97–105. Available at: <http://doi.org/10.4103/2321-3868.132689>
- Strnad P, Tacke F, Koch A, Trautwein C. Liver – guardian, modifier and target of sepsis. *Nat Rev Gastroenterol Hepatol*. 2016;14(1):55–66. Available at: <http://doi.org/10.1038/nrgastro.2016.168>
- Chen YN, Hu MR, Wang L, Chen WD. Macrophage M1/M2 polarization. *Eur J Pharmacol*. 2020;877:173090. Available at: <http://doi.org/10.1016/j.ejphar.2020.173090>
- Shapouri-Moghaddam A, Mohammadian S, Vazini H, et al. Macrophage plasticity, polarization, and function in health and disease. *J Cell Physiol*. 2018;233(9):6425–6440. Available at: <http://doi.org/10.1002/jcp.26429>
- Kadomoto S, Izumi K, Mizokami A. Macrophage polarity and disease control. *Int J Mol Sci*. 2021;23(1):144. Available at: <http://doi.org/10.3390/ijms23010144>
- Fang HL, Chen J, Luo J, et al. Abietic acid attenuates sepsis-induced lung injury by inhibiting nuclear factor kappa-light-chain-enhancer of activated B cells (NF- $\kappa$ B) pathway to inhibit M1 macrophage polarization. *Exp Anim*. 2022;71(4):481–490. Available at: <http://doi.org/10.1538/expanim.22-0018>
- Fink MP, Warren HS. Strategies to improve drug development for sepsis. *Nat Rev Drug Discov*. 2014;13(10):741–758. Available at: <http://doi.org/10.1038/nrd4368>
- Rhee C, Kadri SS, Dekker JP, et al. Prevalence of antibiotic-resistant pathogens in culture-proven sepsis and outcomes associated with inadequate and broad-spectrum empiric antibiotic use. *JAMA Netw Open*. 2020;3(4):e202899. Available at: <http://doi.org/10.1001/jamanetworkopen.2020.2899>
- Manvar D, Mishra M, Kumar S, Pandey VN. Identification and evaluation of anti Hepatitis C virus phytochemicals from *Eclipta alba*. *J Ethnopharmacol*. 2012;144(3):545–554. Available at: <http://doi.org/10.1016/j.jep.2012.09.036>
- Lu Y, Hu DM, Ma SB, et al. Protective effect of wedelolactone against CCl<sub>4</sub>-induced acute liver injury in mice. *Int Immunopharmacol*. 2016;34:44–52. Available at: <http://doi.org/10.1016/j.intimp.2016.02.003>
- Wang MQ, Zhang KH, Liu FL, et al. Wedelolactone alleviates cholestatic liver injury by regulating FXR-bile acid-NF- $\kappa$ B/NRF2 axis to reduce bile acid accumulation and its subsequent inflammation and oxidative stress. *Phytomedicine*. 2024;122:155124. Available at: <http://doi.org/10.1016/j.phymed.2023.155124>
- Yuan F, Chen J, Sun PP, et al. Wedelolactone inhibits LPS-induced pro-inflammation via NF-kappaB pathway in RAW 264.7 cells. *J Biomed Sci*. 2013;20(1):84. Available at: <http://doi.org/10.1186/1423-0127-20-84>
- Lin JY, Lai YS, Liu CJ, Wu AR. Effects of lotus plumule supplementation before and following systemic administration of lipopolysaccharide on the splenocyte responses of BALB/c mice. *Food Chem Toxicol*. 2007;45(3):486–493. Available at:

21. <http://doi.org/10.1016/j.fct.2006.09.012>
21. Liu AC, Patel K, Vunikili RD, et al. Sepsis in the era of data-driven medicine: personalizing risks, diagnoses, treatments and prognoses. *Brief Bioinform.* 2019;21(4):1182–1195. Available at: <http://doi.org/10.1093/bib/bbz059>
22. Opal SM, Garber GE, LaRosa SP, et al. Systemic host responses in severe sepsis analyzed by causative microorganism and treatment effects of drotrecogin alfa (activated). *Clin Infect Dis.* 2003;37(1):50–58. Available at: <http://doi.org/10.1086/375593>
23. Francis MR, El-Sheakh AR, Suddek GM. Saroglitazar, a dual PPAR- $\alpha/\gamma$  agonist, alleviates LPS-induced hepatic and renal injury in rats. *Int Immunopharmacol.* 2023;115:109688. Available at: <http://doi.org/10.1016/j.intimp.2023.109688>
24. Wen Y, Lambrecht J, Ju C, Tacke F. Hepatic macrophages in liver homeostasis and diseases-diversity, plasticity and therapeutic opportunities. *Cell Mol Immunol.* 2021;18(1):45–56. Available at: <http://doi.org/10.1038/s41423-020-00558-8>
25. Tacke F. Targeting hepatic macrophages to treat liver diseases. *J Hepatol.* 2017;66(6):1300–1312. Available at: <http://doi.org/10.1016/j.jhep.2017.02.026>
26. Yan J, Li S, Li SL. The role of the liver in sepsis. *Int Rev Immunol.* 2014;33(6):498–510. Available at: <http://doi.org/10.3109/08830185.2014.889129>
27. Liang XJ, Li TY, Zhou QC, et al. Mesenchymal stem cells attenuate sepsis-induced liver injury via inhibiting M1 polarization of Kupffer cells. *Mol Cell Biochem.* 2019;452(1–2):187–197. Available at: <http://doi.org/10.1007/s11010-018-3424-7>
28. Wang SY, Liu RC, Yu Q, Dong L, Bi YJ, Liu GW. Metabolic reprogramming of macrophages during infections and cancer. *Cancer Lett.* 2019;452:14–22. Available at: <http://doi.org/10.1016/j.canlet.2019.03.015>
29. Sun YY, Li XF, Meng XM, Huang C, Zhang L, Li J. Macrophage phenotype in liver injury and repair. *Scand J Immunol.* 2017;85(3):166–174. Available at: <http://doi.org/10.1111/sji.12468>
30. Wang C, Ma C, Gong LH, et al. Macrophage polarization and its role in liver disease. *Front Immunol.* 2021;12:803037. Available at: <http://doi.org/10.3389/fimmu.2021.803037>
31. Wu MM, Wang QM, Huang BY, et al. Dioscin ameliorates murine ulcerative colitis by regulating macrophage polarization. *Pharmacol Res.* 2021;172:105796. Available at: <http://doi.org/10.1016/j.phrs.2021.105796>
32. Xue MT, Sheng WJ, Song X, et al. Atractylenolide III ameliorates spinal cord injury in rats by modulating microglial/macrophage polarization. *CNS Neurosci Ther.* 2022;28(7):1059–1071. Available at: <http://doi.org/10.1111/cns.13839>
33. Wang Z, Zhang XX, Zhu LL, et al. Inulin alleviates inflammation of alcoholic liver disease via SCFAs-inducing suppression of M1 and facilitation of M2 macrophages in mice. *Int Immunopharmacol.* 2020;78:106062. Available at: <http://doi.org/10.1016/j.intimp.2019.106062>
34. Sha WJ, Zhao B, Wei HZ, et al. Astragalus polysaccharide ameliorates vascular endothelial dysfunction by stimulating macrophage M2 polarization via potentiating Nrf2/HO-1 signaling pathway. *Phytomedicine.* 2023;112:154667. Available at: <http://doi.org/10.1016/j.phymed.2023.154667>
35. Zhao MH, Li C, Shen FJ, Wang MJ, Jia N, Wang CB. Naringenin ameliorates LPS-induced acute lung injury through its anti-oxidative and anti-inflammatory activity and by inhibition of the PI3K/AKT pathway. *Exp Ther Med.* 2017;14(3):2228–2234. Available at: <http://doi.org/10.3892/etm.2017.4772>
36. Zhang BB, Zeng MN, Li BK, et al. Arbutin attenuates LPS-induced acute kidney injury by inhibiting inflammation and apoptosis via the PI3K/Akt/Nrf2 pathway. *Phytomedicine.* 2021;82:153466. Available at: <http://doi.org/10.1016/j.phymed.2021.153466>
37. Zhong WH, Qian KJ, Xiong JB, Ma K, Wang AZ, Zou Y. Curcumin alleviates lipopolysaccharide induced sepsis and liver failure by suppression of oxidative stress-related inflammation via PI3K/AKT and NF- $\kappa$ B related signaling. *Biomed Pharmacother.* 2016;83:302–313. Available at: <http://doi.org/10.1016/j.biopha.2016.06.036>
38. Hyam SR, Lee IA, Gu W, et al. Arctigenin ameliorates inflammation in vitro and in vivo by inhibiting the PI3K/AKT pathway and polarizing M1 macrophages to M2-like macrophages. *Eur J Pharmacol.* 2013;708(1–3):21–29. Available at: <http://doi.org/10.1016/j.ejphar.2013.01.014>
39. O'Dea E, Hoffmann A. NF- $\kappa$ B signaling. *Wiley Interdiscip Rev Syst Biol Med.* 2009;1(1):107–115. Available at: <http://doi.org/10.1002/wsbm.30>
40. Zhang YD, Cheng J, Su YF, Li MY, Wen J, Li SX. Cordycepin induces M1/M2 macrophage polarization to attenuate the liver and lung damage and immunodeficiency in immature mice with sepsis via NF- $\kappa$ B/p65 inhibition. *J Pharm Pharmacol.* 2022;74(2):227–235. Available at: <http://doi.org/10.1093/jpp/rgab162>